Implementation of track length estimator for flux distribution tallies using proper orthogonal decomposition in one-dimensional geometry

Ryoichi Kondo[1*], *Tomohiro* Endo[2], and *Akio* Yamamoto[2]

[1]Japan Atomic Energy Agency, 2-4 Shirakata, Tokai-mura, Naka-gun, Ibaraki, 319-1195, Japan
[2] Nagoya University, Furo-cho, Chikusa-ku, Nagoya, 464-8603, Japan

Abstract. In a recent study, we have developed an efficient flux distribution tallying method in the Monte Carlo calculation toward the high-fidelity, large scale multi-physics simulation. In this method, the proper orthogonal decomposition is applied to the flux distribution tallies. While the tallying method was implemented with the collision estimator in the previous study, the track length estimator is implemented in the present study to obtain the tally with lower statistical error. The implementation of the flux distribution tally with the track length estimator is compared with that of the collision estimator and the normal track length estimator in a one-dimensional problem. The numerical results reveal that the distribution tally using the proper orthogonal decomposition with the track length estimator can obtain a more precise solution compared with that with the collision estimator. Therefore, in terms of the statistical error, the relationship between the distribution tally with track length and collision estimators is similar to that between the conventional track length and collision estimators.

1 Introduction

A high-fidelity, large scale multi-physics simulation with the Monte Carlo (MC) neutronics calculation [1–4] has been available due to the high-performance computing. The neutronics calculation has the role of calculating the power distribution transferred to other physics calculations (e.g., thermal-hydraulics and fuel performance). However, there are the following issues with treating the finely discretized distribution by the MC method. One is a data transfer of the detailed large scale distribution. The other is to reduce the statistical error in each mesh of the distribution due to the trade-off between the computational resource and the statistical error.

The proper orthogonal decomposition (POD) [5] is an approach to reduce dimensionality (the degrees of freedom) and has been applied to neutronics calculations in recent studies [6–9]. To address the issues described above, we have developed a flux distribution tallying method using the POD [9]. In this method, the target spatial flux distribution is expanded by the orthogonal basis vectors. The basis vectors are extracted from the pre-calculated snapshot by using the singular value decomposition (SVD). The expansion coefficient is tallied during

* Corresponding author: kondo.ryoichi@jaea.go.jp

the random walk of the MC calculation. The dimensionality of the flux distribution is reduced from the number of meshes to the POD expansion order. The total statistical error of flux distribution increases monotonically with respect to the POD expansion order. As the POD expansion order becomes lower, the statistical error can be reduced.

In the previous study [9], the collision estimator was used to tally the expansion coefficient since the implementation was straightforward. Typically, the statistical error of the track length estimator is lower than that of the collision estimator in most problems, especially the geometry including the materials with small total macroscopic cross sections. To address the open issue in the previous study, we aim to implement the track length estimator in tallying the POD expansion coefficient.

The remainder of this paper is organized into the following sections. A methodology for the flux distribution tallies using the POD and the implementation of the track length estimator are described in Section 2. The present implementation is verified, and the different estimators are compared in Section 3. The concluding remarks are summarized in Section 4.

2 Methodology

2.1 Flux distribution tallies using POD

In this subsection, flux distribution tallies using the POD we developed [9] are briefly described. A target distribution $\boldsymbol{\varphi} \in \mathbb{R}^{R\times 1}$ consisting of R mesh averaged fluxes is assumed to be expanded by the linear combination of N orthogonal basis vectors as follows:

$$\boldsymbol{\varphi} = (\varphi_1 \quad \varphi_2 \quad \cdots \quad \varphi_R)^{\mathrm{T}} = \mathbf{U}\mathbf{a}, \tag{1}$$

where

$$\mathbf{U} = (\mathbf{u}_1 \quad \mathbf{u}_2 \quad \cdots \quad \mathbf{u}_N), \mathbf{a} = (a_1 \quad a_2 \quad \cdots \quad a_N)^{\mathrm{T}}. \tag{2}$$

$\mathbf{u}_i \in \mathbb{R}^{R\times 1}$ and a_i are the i-th orthonormal basis vector and the i-th expansion coefficient, respectively, and T denotes the transpose. The expansion coefficient is obtained as the following equation using the orthonormality of the basis vectors.

$$\mathbf{a} = \mathbf{U}^{\mathrm{T}}\boldsymbol{\varphi} \tag{3}$$

During the random walk of the MC calculation, the expansion coefficient is tallied by using the right-hand side of Equation (3). The target distribution is reconstructed using Equation (1) with the tallied expansion coefficient at the end of the MC calculation. The dimensionality of the flux distribution is reduced from the number of tally regions R to the number of expansion coefficients N (the POD expansion order).

The total statistical error of the flux distribution is estimated by the l^2-norm based standard deviation $\|\boldsymbol{\sigma}_\varphi\|$ as the following equation [9].

$$\|\boldsymbol{\sigma}_\varphi\| = \sqrt{\sum_{r=1}^{R} \sigma_{\varphi_r}^2} = \sqrt{\sum_{n=1}^{N} \sigma_{a_n}^2}, \tag{4}$$

where $\sigma_{\varphi_r}^2$ and $\sigma_{a_n}^2$ are the variance of flux in the tally region r and the variance of the n-th expansion coefficient. As shown in Equation (4), the l^2-norm based standard deviation is calculated from the summation of the variances for the expansion coefficient. It increases monotonically with respect to the POD expansion order. If the POD expansion order is sufficiently low, the statistical error of the flux distribution can be reduced. It is noted that the POD expansion order should be high enough to avoid the increase in the truncation error of POD.

In the present study, the pre-calculated mesh average flux is used as the snapshot flux distribution to obtain the basis vectors. The calculation conditions for the snapshot are chosen in such that the snapshot captures the characteristics of the target distribution. For example, macroscopic cross section [6], atomic number density [8], or albedo value [9] is perturbed for the snapshot calculation. In the verification of Section 3, the snapshots with various albedo values are calculated by the method of characteristics (MOC). The snapshot matrix $\mathbf{\Phi} \in \mathbb{R}^{R\times S}$ consisting of S mesh averaged fluxes is decomposed by the SVD as the following equation.

$$\mathbf{\Phi} = (\boldsymbol{\varphi}_1 \quad \boldsymbol{\varphi}_2 \quad \cdots \quad \boldsymbol{\varphi}_S) = \mathbf{U\Sigma V}^{\mathrm{T}}. \tag{5}$$

The first N orthogonal basis vectors ($N < S$) in the left singular vectors $\mathbf{U} \in \mathbb{R}^{R\times S}$ are used to expand the target flux distribution. The deterministic method is used to obtain the snapshots [8, 9] because the preliminary study reveals the basis vector extracted from the snapshot obtained by the MC method is degraded due to the statistical error of the snapshot.

2.2 Implementation of track length estimator

In the normal flux tallies with the track length estimator, the mesh averaged flux φ_r is tallied as follows:

$$\varphi_r = \frac{1}{V_r}\frac{1}{H}\sum_{h=1}^{H} D_{r,h}, \tag{6}$$

$$D_{r,h} = \sum_{k=1}^{K_h} d_{r,h,k} w_{r,h,k}, \tag{7}$$

where $d_{r,h,k}$ and $w_{r,h,k}$ are the track length and weight of the history h passing through the tally region r between the k-th and $(k+1)$-th events, respectively. V_r, H, and K_h are the volume of the tally region r, the total number of histories, and the total number of events for the history h, respectively.

In the flux distribution tallies using the POD, the expansion coefficient is tallied by Equation (3) during the random walk of the MC calculation. The n-th expansion coefficient is obtained by substituting Equation (6) into Equation (3) as follows:

$$a_n = \mathbf{u}_n^{\mathrm{T}}\boldsymbol{\varphi} = \sum_{r=1}^{R}\left(u_{n,r}\varphi_r\right) = \frac{1}{H}\sum_{h=1}^{H}\sum_{r=1}^{R}\left(\frac{u_{n,r}D_{r,h}}{V_r}\right), \tag{8}$$

where $u_{n,r}$ is the element of the n-th basis vector in the tally region r. In the implementation, $u_{n,r}D_{r,h}$ is not always calculated since $D_{r,h}$ is zero when the history h does not pass through the tally region r. Although the collision estimator counts the contribution of a neutron to the basis vector corresponding to one mesh where a neutron collided, the track length estimator can count the contribution to the basis vector corresponding to the multiple meshes where a neutron passes through. Hence the statistical error of the expansion coefficient obtained by the track length estimator can be lower than that by the collision estimator.

3 Numerical calculations

3.1 Calculation conditions

A one-dimensional slab geometry in Figure 1 is used to verify the implementation of the flux distribution tally using the POD with the track length estimator. The one energy group eigenvalue Monte Carlo calculation is carried out with the macroscopic cross sections in Table 1. The macroscopic cross sections are created from the three compositions listed in the VERA benchmark problems [10], with the option to output the macroscopic cross section in the continuous energy MC code MVP3 [11]. The slab geometry of 10 cm is equally divided into 100 meshes. The mesh averaged fluxes are calculated as the target flux distribution in space.

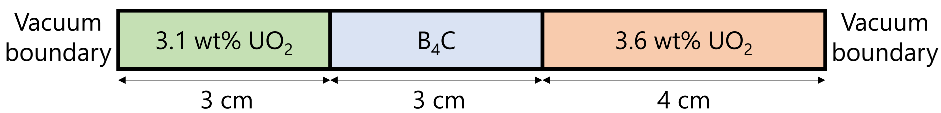

Fig. 1. One-dimensional slab geometry.

Table 1. One energy group macroscopic cross sections.

Material	**3.1 wt% UO_2**	**3.6 wt% UO_2**	**B_4C**
Σ_a [cm^{-1}]	7.26982E-03	7.39679E-03	1.48649E-02
$\nu\Sigma_f$ [cm^{-1}]	1.20949E-02	1.25005E-02	0.00000E+00
Σ_t [cm^{-1}]	3.47921E-01	3.46872E-01	3.05995E-01
Σ_s [cm^{-1}]	3.40651E-01	3.39475E-01	2.91130E-01
χ [-]	1.0	1.0	0.0

To generate the basis vectors, the mesh averaged fluxes in the slab geometry with various conditions are calculated as the snapshots. In the present study, by perturbing the atomic densities (macroscopic cross sections) of the three materials separately using four fractions (±10, ±20%), 64 (= 4^3) different conditions are prepared. The snapshots are obtained by the MOC using the GENESIS code [12]. The size of the snapshot matrix is 100×64 and 64 orthogonal basis vectors are extracted by the SVD.

The target flux distribution is calculated by a single energy group in-house MC code. Four estimators are used: (a) POD track length estimator (the present implementation), (b) POD collision estimator, (c) normal track length estimator, and (d) normal collision estimator. In the "normal estimator," the mesh averaged flux itself is tallied. On the other hand, in the "POD estimator," the expansion coefficient corresponding to the basis vector is tallied and the flux distribution is reconstructed at the end of the MC calculation. To estimate the statistical error, one hundred independent calculations are carried out for each estimator.

The reference mesh averaged flux is calculated by the track length estimator of the multi-group MC code GMVP [11] with a sufficiently large number of histories. The number of histories for each MC calculation is shown in Table 2. The number of inactive batches is set to sufficiently converge the fission source distribution. The number of active batches for in-house code is set so that the relative standard deviation of the flux distribution obtained by the normal collision estimator is less than 0.2%. For the reference GMVP calculation, the number of active batches is set to achieve the relative standard deviation of the flux distribution that is approximately one-hundredth of that obtained by the normal collision estimator of in-house code (~ 0.0025% at maximum).

Table 2. Number of histories for the MC calculations.

	In-house code	**GMVP**
Number of histories per batch	10,000	10,000
Number of inactive batches	200	200
Number of active batches	1,000	1,000,000

3.2 Results and discussion

First, to verify the present implementation, the mesh averaged flux obtained from the POD track length estimator is compared with the reference GMVP solution. The relative difference of the mesh averaged flux is shown in Figure 2. The POD expansion order is seventh when the accuracy of the entire flux distribution is sufficient from the following discussion of Figure 4. The result of the POD track length estimator agrees with the reference within one standard deviation.

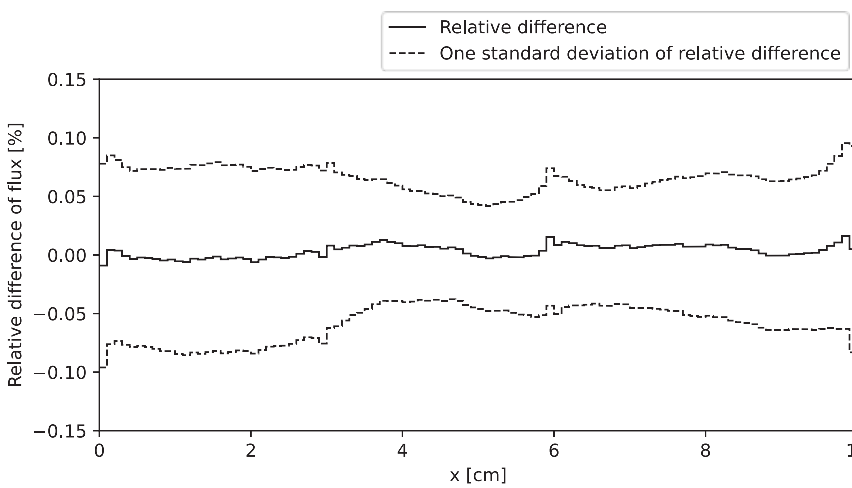

Fig. 2. Relative difference of flux between the POD track length estimator and the reference. The POD expansion order is seventh.

Second, the tallied expansion coefficient obtained by the POD track length and collision estimators is compared. The absolute value of the expansion coefficient is shown in Figure 3. The statistical error is obtained by processing the results of one hundred independent MC calculations. The first six coefficients could be effective in reconstructing the target distribution since the coefficients after the sixth are too small and their statistical error is large. Table 3 shows the mean and standard deviation of the expansion coefficient from the first to the tenth. As observed from the first to the sixth, the statistical error of the POD track length estimator is lower than that of the POD collision estimator. This relationship between the POD estimators is similar to that of the statistical error between normal track length and collision estimators. After the sixth, the expansion coefficient is statistically insignificant due to the larger magnitude of the statistical error relative to the mean.

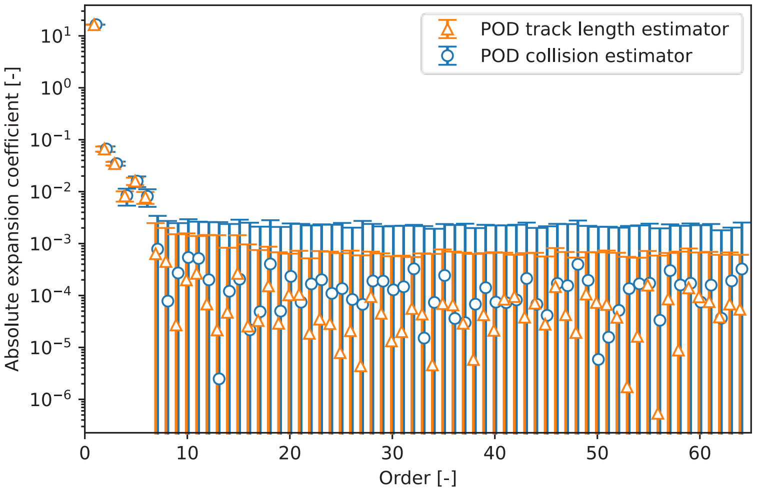

Fig. 3. Absolute expansion coefficient. Error bar means one standard deviation.

Table 3. Expansion coefficient from the first to the tenth.

Order	POD track length estimator		POD collision estimator	
	Mean value [-]	Standard deviation [-]	Mean value [-]	Standard deviation [-]
1	1.6E+01	4.4E-03	1.6E+01	4.8E-03
2	-6.6E-02	7.4E-03	-6.6E-02	8.2E-03
3	-3.5E-02	2.7E-03	-3.5E-02	3.2E-03
4	-8.3E-03	1.9E-03	-8.4E-03	3.0E-03
5	-1.6E-02	2.6E-03	-1.6E-02	3.7E-03
6	-7.8E-03	2.0E-03	-8.1E-03	3.0E-03
7	6.4E-04	1.8E-03	7.8E-04	2.6E-03
8	-4.5E-04	1.5E-03	7.8E-05	2.7E-03
9	2.7E-05	1.5E-03	-2.7E-04	2.2E-03
10	2.0E-04	1.4E-03	5.4E-04	2.4E-03

Third, the accuracy of the entire flux distribution is discussed. The systematic error of the flux distribution is estimated by relative root mean square error (RMSE) as follows:

$$\mathrm{RMSE} = \sqrt{\frac{\sum_{r=1}^{R}\left((\varphi_{calc,r}-\varphi_{ref,r})/\varphi_{ref,r}\right)^2}{R}},\ \varphi_{calc,r} = \frac{1}{C}\sum_{c=1}^{C}\varphi_{calc,r,c}, \tag{9}$$

where $\varphi_{calc,r}$ is the mesh averaged flux in the tally region r obtained by the c-th MC calculation of the in-house code, $\varphi_{ref,r}$ is the mesh averaged flux in the tally region r obtained by the reference GMVP code, $R(=100)$ is the total number of tally regions, and $C(=100)$ is the total number of independent MC calculations. Note that RMSE includes statistical error since $\varphi_{calc,r}$ and $\varphi_{ref,r}$ are obtained by the MC calculations. RMSE against the POD expansion order is shown in Figure 4. RMSE obtained by the normal estimator does not depend on the POD expansion order since the flux is not expanded by the basis vectors.

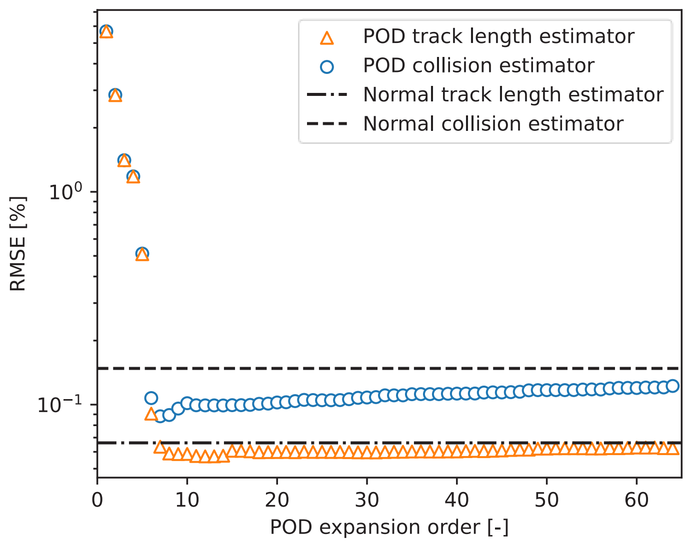

Fig. 4. RMSE of the flux distribution against the POD expansion order.

As shown in Figure 4, the POD track length estimator achieves the accuracy of the normal track length estimator when the POD expansion order is seventh. The dimensionality of the flux distribution is reduced from one hundred (the total number of meshes) to seven (the POD expansion order) for the track length estimator (one hundred to six for the collision estimator). For both track length and collision estimator, the RMSE of the POD estimator decreases exponentially against the POD expansion order and converges to the RMSE of the normal estimator after reaching a minimum value. The trend appears because the truncation error decreases and the statistical error increases against the POD expansion order. The POD expansion order when the RMSE is minimized for the POD track length estimator (twelfth) is higher than that for the POD collision estimator (seventh). This is because the increase in the statistical error for the POD track length estimator is smaller than that for the POD collision estimator as shown in Figure 5. In other words, the POD track length estimator can obtain a more accurate solution compared with the POD collision estimator with the same POD expansion order.

Finally, the statistical error of the POD estimator is discussed. The total statistical error of the flux distribution is estimated by the l^2-norm based standard deviation as follows:

$$\|\boldsymbol{\sigma}_{\varphi}\| = \sqrt{\sum_{r=1}^{R} \sigma_{\varphi_r}^2} = \sqrt{\sum_{r=1}^{R} \left(\frac{1}{C-1} \sum_{c=1}^{C} \left(\varphi_{calc,r,c} - \varphi_{calc,r} \right)^2 \right)}, \tag{10}$$

where $\sigma_{\varphi_r}^2$ is the variance of the mesh averaged flux in tally region r. l^2-norm based standard deviation against the POD expansion order is shown in Fig 5. l^2-norm based standard deviation obtained by the normal estimator does not depend on the POD expansion order.

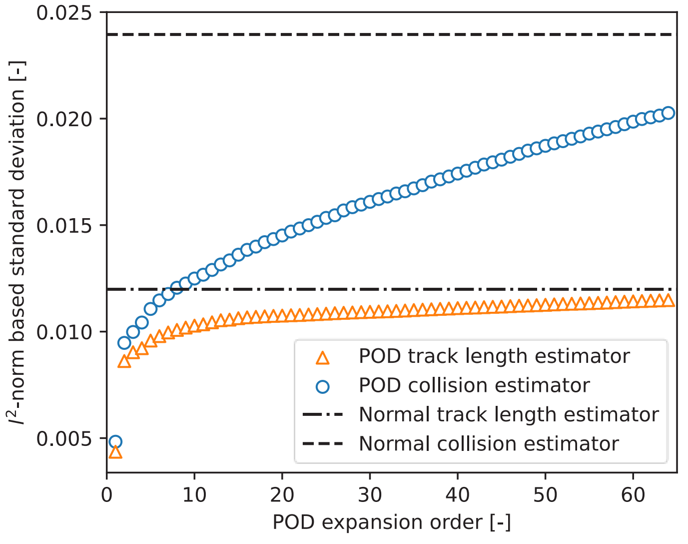

Fig. 5. l^2-norm standard deviation against the POD expansion order.

As shown in Figure 5, the l^2-norm standard deviation of the POD estimator is increased monotonically. Thanks to this feature of the POD estimator, the statistical error of the flux distribution can be reduced, if the POD expansion order is sufficiently low, as mentioned in Section 2.1. The percent reduction in l^2-norm based standard deviation of the POD estimator compared with the normal estimator is shown in Table 4. The POD expansion order is chosen so that the RMSE of the POD estimator is below that of the normal estimator for the first time starting from the first order (seventh and sixth for the track length and collision estimators, respectively). The reduction in statistical error of the POD track length estimator is smaller than that of the POD collision estimator. The reason for this is that the present problem is convenient for the normal track length estimator since the mean free path (~ 3 cm) is relatively large for the geometry size (10 cm). The reduction of l^2-norm standard deviation could be larger in the problem with large geometry for the track length estimator. When comparing two POD estimators, the l^2-norm standard deviation of the POD track length estimator is lower than that of the POD collision estimator as shown in Figure 5. Consequently, the POD track length estimator can obtain a more precise solution compared with the POD collision estimator.

Table 4. Percent reduction of the l^2-norm standard deviation from the normal estimator.

Estimator	POD expansion order	Reduction of l^2-norm standard deviation from POD estimator to normal estimator
Track length estimator	7	17%
Collision estimator	6	52%

4 Conclusions

We have developed the tallying method using the POD to calculate the finely discretized flux distribution in a recent study. In the present study, the track length estimator is newly utilized to calculate the flux distribution instead of the collision estimator used in the previous study. The implementation is verified in the one-dimensional slab geometry. The "POD track length estimator" can tally the flux distribution with lower statistical error compared with the "POD collision estimator." This relationship between the POD estimators is similar to that of statistical error between the "normal" track length and collision estimators.

The following items are planned for future tasks. First, the tally using the POD will be applied to more practical problems, e.g., two- or three-dimensional complex geometry of unstructured meshes with tens to hundreds of energy groups. The performance including the calculational time of the present approach will be investigated on those problems. Second, an efficient methodology to prepare the snapshot (e.g., data augmentation) will also be investigated since the generation of the snapshot could require additional computation resources. Finally, an efficient data transfer of the distribution quantities will be demonstrated in the multi-physics simulation as a final goal of this study.

References

1. M. Ellis, D. Gaston, B. Forget, K. Smith, Nucl. Sci. Eng., **185**, 184 (2017)
2. K. Wang, S. Liu, Z. Li, G. Wang, J. Liang, F. Yang, Z. Chen, X. Guo, Y. Qiu, Q. Wu, J. Guo, X. Tang, Prog. Nucl. Energy., **98**, 301 (2017)
3. A. J. Novak, D. Andrs, P. Shriwise, J. Fang, H. Yuan, D. Shaver, E. Merzari, P. K. Romano, R. C. Martineau, Ann. Nucl. Energy., **177**, 109310 (2022)
4. K. Tada, R. Kondo, T. Kamiya, T. Nagatake, A. Ono, Y. Nagaya, H. Yoshida, *Development of High-Fidelity Multi-Physics Platform JAMPAN*, in Proceedings of International Conference on Physics of Reactors, PHYSOR, 21-24 Apr. 2024, San Francisco, CA, US (2024)
5. J. S. R. Anttonen, P. I. King, P. S. Beran, Math. Comput. Model., **38**, 41 (2003)
6. P. Behne, J. Vermaak, J. C. Ragusa, J. Comput. Phys., **469**, 111525 (2022)
7. K. Tsujita, T. Endo, A. Yamamoto, J. Nucl. Sci. Technol., **60**, 343 (2023)
8. K. Mori, A. Yamamoto, T. Endo, *Deep Penetration Calculations Combining Proper Orthogonal Decomposition and Monte Carlo Methods*, in Proceedings of International Conference on Mathematics and Computational Methods Applied to Nuclear Science and Engineering, M&C, 13-18 Aug. 2023, Niagara Falls, Ontario, Canada (2023)
9. R. Kondo, T. Endo, A. Yamamoto, Flux Distribution Tallies Using Proper Orthogonal Decomposition in Monte Carlo Calculations, J. Nucl. Sci. Technol. (submitted)
10. A. T. Godfrey, CASL-U-2012-0131-004, Oak Ridge National Laboratory (2014).

11. Y. Nagaya, K. Okumura, T. Sakurai, T. Mori, JAEA-Data/Code 2016-018, Japan Atomic Energy Agency (2017)
12. A. Yamamoto, A. Giho, Y. Kato, T. Endo, Nucl. Sci. Eng. **186**, 1 (2017)